GEOPHYSICAL RESEARCH LETTERS, VOL. 25, NO.12, PAGES 2017-2020, JUNE 15, 1998

# FAST observations in the downward auroral current region: Energetic upgoing electron beams, parallel potential drops, and ion heating

C. W. Carlson[1], J. P. McFadden[1], R. E. Ergun[1], M. Temerin[1], W. Peria[1], F. S. Mozer[1], D. M. Klumpar[2], E. G. Shelley[2], W. K. Peterson[2], E. Moebius[3], R. Elphic[4], R. Strangeway[5], C. Cattell[6], and R. Pfaff[7]

**Abstract.** Observations of plasma particles and fields by the FAST satellite find evidence of acceleration of intense upgoing electron beams by quasi-static parallel electric fields. The beam characteristics include a broad energy spectrum with peak energies between 100 eV and 5 keV, perpendicular temperatures less than 1 eV, and fluxes greater than $10^9$/cm$^2$sec. Diverging electrostatic shocks associated with the beams have integrated potentials that match the beam energy. These beams are found in regions of downward Birkeland current and account for the total field-aligned current when they are present. The most energetic ion conics in the auroral zone are found coincident with these beams, in agreement with the model for "trapped" conics. The measured particle densities of the electron beams and associated ion conics are approximately equal and typically range from 1 to 10 cm$^{-3}$, with no evidence for additional cold density. The beams are seen frequently at altitudes between 2000 and 4000 km in the winter auroral zone. Their probability of occurrence has a strong dependence on season and altitude and is similar to that for upgoing ion beams in the adjacent upward current regions. This similarity suggests that the density and scale height of ionospheric ions play an important role in the formation of both types of beams.

## Introduction

Understanding the origin and nature of parallel potential drops and particle acceleration in the Birkeland current systems remains one of the most intriguing problems in magnetospheric physics. Extensive observations have been made within the upward current regions where ion beams and inverted V electrons originate. *Evans* [1974] showed that auroral electron energy spectra suggested the presence of parallel potential drops. Identification of electrostatic shocks and corresponding ion beams from the S3-3 satellite observations was a key step in demonstrating that parallel electric fields existed in the mid-altitude auroral zone and were responsible for accelerating auroral particles [*Mozer et al.*, 1977, *Shelley et al.*, 1976; *Temerin et al.*, 1981; *Redsun et al.*, 1985]. There are relatively few reports of particle beams and electrostatic shocks in the downward current system. Intense upgoing field-aligned electron beams were reported by *Klumpar and Heikkila* [1982], and more recently by *Boehm et al.* [1995], and upgoing electrons near the cusp have been identified as carriers of downward Birkeland currents [*Burch et al.*, 1983]. *Marklund et al.* [1994] reported intense diverging electrostatic shocks and upgoing electrons associated with "black aurora".

In this paper we present observations made by the high resolution plasma and fields instruments on the FAST satellite and demonstrate that upgoing beams of energetic electrons are not rare but appear with a probability similar to that of ion beams. There is good agreement between the measured potential of diverging shocks and the energy of the corresponding electron beams, and the beam currents show excellent quantitative agreement with the measured magnetic field deflections. Intense energetic ion conics having a distinctive "trapping" signature frequently accompany the electron beams.

## Observations

The FAST satellite is in a 350 by 4200 km altitude orbit with 83° inclination, and has an orbital period of approximately 2 hours. Its spin axis tilts slightly from the orbit normal direction such that the earth's magnetic field is nearly always within 5° of the spin plane during auroral zone passes. The plasma instrumentation includes two pair of "top-hat" electrostatic analyzers to measure the high resolution energy spectra of ions (3 eV-25 keV) and electrons (4 eV-30 keV) in 32 pitch-angle bins every 78 ms. The two analyzers of each pair are mounted on opposite sides of the spacecraft with their 180° fields-of-view lying in the spin plane. Deflection plates automatically steer the view direction to follow the magnetic field, so complete pitch-angle spectra are measured every energy sweep, independent of the spacecraft spin. Pitch-angle and energy bins are contiguous to ensure that no fine angle or energy features of beams are missed. A summary of FAST instruments is found in the overview paper for this special section [*Carlson et al.*, 1998].

Figure 1 shows high time resolution observations from an active northern auroral crossing near magnetic midnight. This event was selected because it has clearly defined regions of upward and downward current and illustrates a wide range of characteristic auroral features during a single auroral crossing. The top panel displays the spin axis component (nearly westward) of the perturbation magnetic field (**B** - model **B**). The negative slope of this trace indicates an upward Birkeland current throughout the first half of the pass, which then reverses, showing that a more intense and structured downward current existed throughout the northern half of the pass. This pattern matches the statistical region 1 and 2 current systems expected near midnight [*Ijima and Potemra*, 1978].

Electron data are displayed in the next 5 panels. Panels (b) and (d) are energy-time spectrograms for upgoing and downgoing electrons and panel (c) is the corresponding pitch-angle spectrogram with 0° corresponding to downgoing fluxes. The total upgoing and downgoing particle and energy fluxes are shown in panels (e) and (f). A broad region of inverted V elec-

[1]Space Science Laboratory, University of California, Berkeley
[2]Lockheed Martin Palo Alto Research Laboratory, Palo Alto, CA
[3]University of New Hampshire, Durham, NH
[4]Los Alamos National Laboratory, Los Alamos, NM
[5]IGPP, University of California, Los Angeles
[6]University of Minnesota, Minneapolis
[7]Goddard Space Flight Center, Greenbelt, MD



Paper number 98GL00851.
0094-8534/98/98GL-00851$05.00

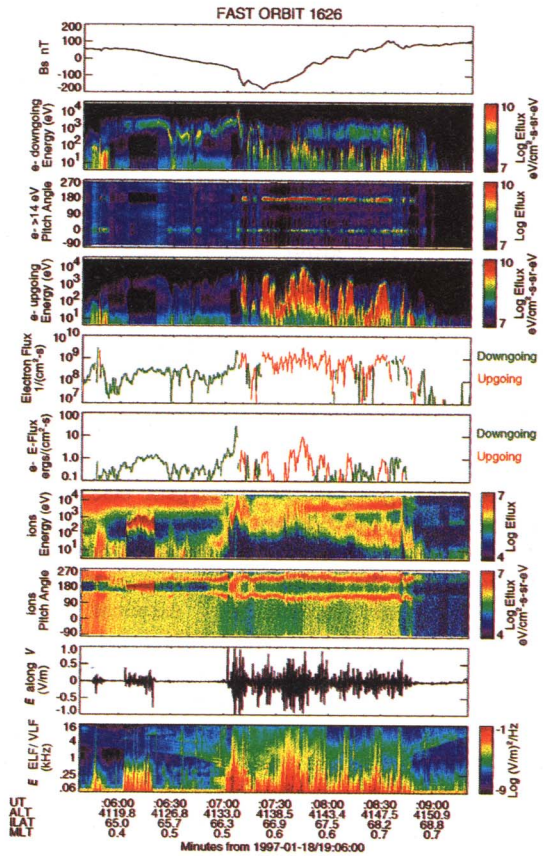


**Figure 1.** FAST observations of an auroral crossing near magnetic midnight that has nearly equal width regions of upward and downward Birkeland currents. Panels, starting from top: (a) The spin axis component (nearly westward) of the magnetic field. A positive (negative) slope indicates downward (upward) current. (b ,c, d) Electron energy flux spectrograms versus energy and pitch angle. Fluxes near 180° are upgoing. (e, f) Total electron particle flux and energy flux, color coded for upgoing (green), and downgoing (red). (g, h) Ion energy flux spectrograms versus energy and pitch angle. The energy spectrogram is for all pitch angles. (i) The DC electric field signal perpendicular to **B** and parallel to the spacecraft velocity. (j) Power spectral density of low frequency E-field.

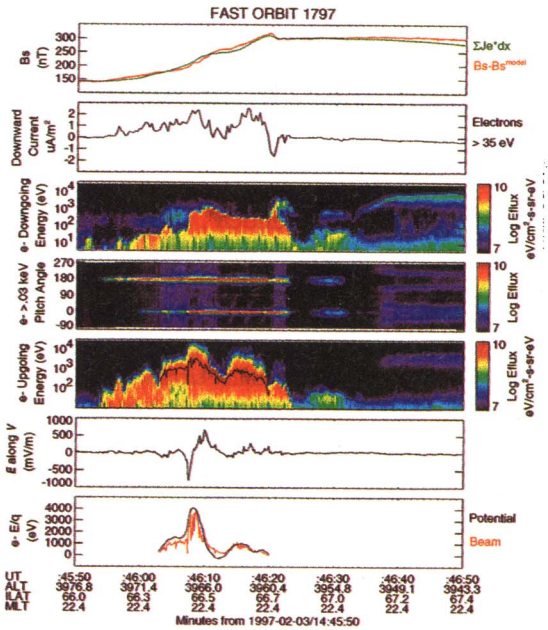


**Figure 2.** Quantitative comparisons of measured magnetic field perturbations and electric potentials with their corresponding electron signatures in an upgoing beam event. Panels: (a) Measured change of westward **B** field component (red) compared with field expected from a current sheet modeled from the measured electron current. (b) Current carried by electrons having energies between 35 eV and 30 keV. (c, d, e) Electron energy flux spectrograms. The black overlay trace on the upgoing electron spectrogram denotes the "characteristic energy". (f) The electric field component perpendicular to **B** and parallel to the spacecraft velocity. (g) The parallel potential drop inferred from the integrated electric field compared with the characteristic energy of the electron beam (linear scale).

tron precipitation with an energy peak near 1 keV fills the upward current region (19:06:00 - 19:07:10 UT). This example represents a moderate intensity aurora, with particle fluxes of 2-3x$10^8$ ($cm^2$-s) and a peak energy flux of 1 erg/$cm^2$-s, except for the narrow region of 10 erg/$cm^2$-s at its northern edge. The spectrogram color exaggerates the impression that the inverted V has low intensity because the color scale runs from $10^7$ to $10^{10}$ eV/$cm^2$-sr-s-eV to accommodate the intense fluxes of upgoing electrons in the adjacent downward current region.

The upgoing electrons (located between 19:07:20 UT and the polar cap boundary at ~19:09:00 UT) have peak differential energy fluxes ranging between $10^{10}$ and $10^{11}$ eV/$cm^2$-sr-s-eV, about 100 times greater than typical inverted V differential fluxes. The beam's energy spectrum is very broad, extending from the lowest channel at 4 eV up to an abrupt high energy cutoff near 1 keV, and demonstrates large spatial and/or temporal variations. A weaker and less energetic population of counterstreaming precipitating fluxes is also present. Both of the counterstreaming electron populations have similar narrow pitch angles with perpendicular temperatures less than 1 eV. The upward beams carry typical fluxes of $10^9$/$cm^2$-s, about three to five times greater than in the inverted V, and also have a substantial upward energy flux, peaking at 5 ergs/$cm^2$-s. The measured density of beam electrons varied between 3 and 6 electrons/$cm^3$. No evidence for significant additional cold density was found.

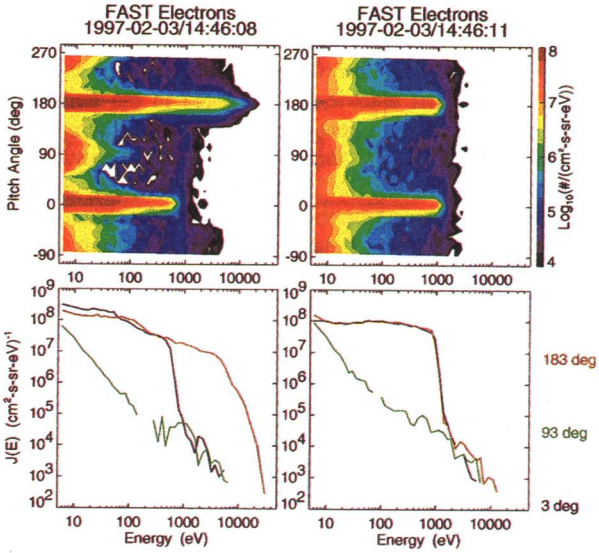


**Figure 3.** Pitch-angle spectrograms (upper panels) and energy spectra (lower panels) for two selected times during the event shown in Fig. 3. The three energy spectra traces are for pitch angles near 0°, 90° and 180°.

The ion and electric field measurements also show distinctively different properties between the upward and downward current regions. In addition to a steady drizzle of hot isotropic plasmasheet ions, the ion spectrograms (panels (g) and (h)) show that the spacecraft crossed an upgoing ion beam at 19:06:02, suggesting that the electrostatic shock potential responsible for the ion acceleration dipped below the spacecraft altitude in this region. The electric field component perpendicular to **B** and aligned with the spacecraft velocity (approximately northward) is plotted in panel (i). The field is turbulent within the beam, but the observed positive spike inbound and negative spike outbound are the signature of crossing a convergent electrostatic shock. A second, more energetic ion beam is found at the edge of the inverted V at 19:07:03. As demonstrated here, ion beams usually exhibit a moderate width in their energy and pitch-angle distributions, in contrast to the broad energy spread and very collimated pitch angles found in the electron beams. Additional results concerning ion beams observed from FAST are presented *by McFadden et al.* [1998], *Moebius et al.* [1998], and *Ergun et al.* [1998a].

Conics and weak plasmasheet ion precipitation are the most common ion signatures in the downward current regions beginning at 19:07:10 UT. The conics are easily identified from the pitch-angle plot as the two symmetric traces that straddle the loss cone, centered at 180°, whereas plasmasheet ions are isotropic. The energy spectrum contains a fairly constant population of plasmasheet ions at an energy of 5 keV. Conics are the second population, which varies in energy between 10 eV and several keV. The distinctive low energy cutoff of the conic energy spectrum visible in this plot is a unique property of the conics that accompany upward electron beams. This cutoff energy level follows the general trend of the electron beam energy. The conic pitch angle also follows the changes in the energy, shifting toward 90° and 270° with increasing energy. These properties agree with predictions by *Gorney et al.* [1985] for the behavior of ion conics trapped by downward parallel electric fields. The measured hot ion density varied between 2 and 6 ions/cm$^3$ through this region.

The electric fields accompanying the electron beams have very intense low frequency fluctuations, with amplitudes ranging between 0.1 and 1 V/m. When isolated beams are seen, the electric fields have clear diverging electrostatic shock signatures as will be demonstrated below. The intense electric field wave spectrum extends into the ELF and VLF range, as illustrated in panel (j). The strong correlation between broad-band ELF waves and conics confirms the findings of *Andre et al.* [1998]. The clear signature of a VLF saucer seen emanating from each side of the upgoing electron beam region is often observed.

Figure 2 shows an expanded view of measurements in a narrow downward current region on the equatorward edge of the pre-midnight aurora. This isolated beam lends itself to quantitative comparisons between the measured field and particle measurements. The current shown in panel (b) was computed from the measured electron distribution. The spacecraft trajectory crossed nearly normal to the model auroral oval boundary on this pass. The calculated magnetic perturbation expected from a perpendicular transit through a current sheet having the measured intensity is compared with magnetometer measurements in panel (a). The excellent agreement between the calculated and measured fields confirms that the superthermal electrons can account for the total current. *McFadden et al.* [1998] report similar results for upward current events.

The upgoing electron spectrogram shown in panel (e) includes an overlay line plot of its characteristic energy, defined as the ratio of the energy flux to the particle flux of the beam. This quantity represents the average energy that beam electrons gain from passing through a potential. The overlay spans the time when high speed burst data were available. The electric field data in panel (f) shows that a strong diverging electrostatic shock is centered on the beam. The parallel potential displayed in panel (g) was obtained by integrating the observed electric field along the spacecraft trajectory. We also assumed that the parallel field vanished at the edges of the beam and imposed a constant ionospheric electric field to match these boundaries. The good agreement between the characteristic electron energy and electric potential drop throughout this 15-s event supports the conclusion that the beams are accelerated by quasi-static potential structures. Analogous examples of agreement between the electric potential structures and the energy of ion beams are found in *McFadden et al.* [1998] and *Ergun et al.* [1998a]. These results demonstrate a strong similarity between the quasi-static electric field structures that accelerate electron and ion beams, but we also find distinctive differences between the resulting ion and electron distribution functions.

Figure 3 illustrates two examples of electron pitch-angle and energy spectra taken during the event shown in Fig. 2 that show counterstreaming fluxes observed in the upgoing beams. The left panels show the spectrum and pitch-angle distribution in the most energetic part of the beam, where the characteristic energy of the upgoing beam was about 5 keV. The energy spectrum has negative slope at all energies below the peak, and above the peak a hot tail extends to 30 keV. In contrast to this broad distribution, the typical ion beam in Fig. 1 had a nearly monoenergetic spectrum. The pitch-angle spectrogram (top panel) gives a qualitative impression of the narrow pitch angles. More quantitative analysis shows that the perpendicular temperature was no greater than a few eV. The spectrum of the downgoing electrons is very similar to the upgoing beam at low energies, but drops off abruptly above 500 eV. This example is representative of upgoing electron beams seen on FAST. The right hand panels of Fig. 3 show a rather rare example, where the up- and downgoing beams are virtually identical.

## Discussion

Upgoing electron beams appear to be far more prevalent in the FAST data than have been reported from earlier measurements. The likely explanation is improved time resolution and uninterrupted viewing of all pitch angles afforded by the FAST instruments. The similarity between the upgoing electron and ion beams and their association with electrostatic shocks motivates a comparison of their occurrence properties.

The altitude and seasonal dependencies of upgoing electron and ion beams are quite similar. During the winter period from early December 1996 through late February 1997, FAST made 670 orbits through the northern auroral zone at altitudes between 2000 and 4000 km. Of these orbits, upgoing electron beams were observed during 78% of the passes, and ion beams were seen on 70%. The occurrence probability for beams of both species dropped rapidly with decreasing altitude below 2500 km, though much more so for ions. The altitudes below which beam events were very rare (<5% per pass) were about 2000 km for ions and 1500 km for electrons. Ion beams have their highest occurrence probability in the late evening sector. These results agree quite well with an earlier study of S3-3 electrostatic shocks reported by *Bennett et al.* [1983], that found a 75% probability of finding shocks between 2000 and 4000 km in the winter. This probability dropped to 18% for summer passes. A

subsequent study by *Redsun et al.* [1985] compared the occurrence rate of ion beams and conics with shocks. They did not identify upgoing electron beams but classified electrons by whether their spin-averaged energy spectrum maximized at low energy or had a "monoenergetic peak". They found that conics were correlated with the intense unpeaked spectra. In retrospect, it is clear that their classification for unpeaked spectra was a proxy for counterstreaming electron beams.

The similarity in the location and probability for occurrence of the two types of beams gives some hints about their origin. The current carriers in both cases are electrons, but the source populations are radically different. The plasmasheet electrons are hot and fairly tenuous whereas the ionosphere electrons are cold and dense. Although the electrons carry the current, the plasma must also remain quasi-neutral, so the ion distributions ultimately control the location along the flux tube where parallel potentials will form. The seasonal dependence of the low altitude extent of shocks suggests that the ion scale height may regulate the formation of both types of beams.

The electric and magnetic field measurements find that intense "solitary waves" are associated with the electron beams, which modulate the beam energy and may account for the large energy spread in the beams. A companion paper [*Ergun et al.*, 1998b] presents observation of these waves, which are found in 5-10% of beam events when the satellite was apparently in the middle of the parallel electric field region. These solitary waves also create large perpendicular electric field pulses which can stochastically heat ions in qualitative agreement with the observed intense ion heating.

The electron beams play an important role in ionosphere-magnetosphere coupling. These beams are undoubtedly the origin of highly collimated counterstreaming beams that are observed deep in the magnetosphere (see *Klumpar* [1993] for examples and numerous references). The close association of the beams with downward Birkeland current regions suggests that these electrons can be used as "tracer particles" to map the connection of these current systems into the outer magnetosphere.

The similarity of the two components of counterstreaming fluxes suggests that they are temporarily "trapped" on the magnetic flux tube. If the electrostatic structures are truly quasi-static, then the field line potentials will map to the conjugate hemisphere, where they may either map down to the ionosphere or close at higher altitude. If the potentials close at high altitude, the main body of the electron distribution will be electrostatically reflected, while the high energy tail will lose energy but still precipitate, producing the downgoing field-aligned beams that are also commonly seen at low altitudes.

In summary, upgoing electron beams are found to be accelerated by diverging electric field, quasi-static potential structures. Except for the reversed polarity, these structures appear to have properties very similar to the electrostatic shocks responsible for accelerating upgoing ion beams and downgoing inverted V electrons that produce auroral light. Just as the inverted V regions have a rich variety of associated phenomena, such as auroral kilometric radiation, ion cyclotron waves, VLF hiss, ion conics, and ion beams, the downward current region has a complementary set of features, including upgoing electron beams, extremely energetic conics, VLF saucers, and the newly discovered fast solitary waves. The "black aurora" is an optical signature of the diverging shocks when they occur in regions of diffuse aurora and suppress the electron precipitation [*Marklund et al.*, 1994]. For the more general case, the reverse shock regions might be considered the "inverse aurora".

**Acknowledgments.** The authors are indebted to the FAST science and technical team members for a successful mission. This research was conducted under NASA grant NAG5-3596.

## References

Andre, M., et al., Ion energization mechanisms at 1700 km in the auroral region, *J. Geophys. Res.*, in press, 1998.

Bennett, E. L., M. Temerin, and F. S. Mozer, The distribution of auroral electrostatic shocks below 8000-km altitude, *J. Geophys. Res.*, *88*, 7107, 1983.

Boehm, M. H., et al., Observations of an upward-directed electron beam with the perpendicular temperature of the cold ionosphere, *Geophys. Res. Lett.*, *22*, 2103, 1995.

Burch, J. L., P. H. Reiff, and M. Sugiura, Upward electron beams measured by DE-1: a primary source of dayside region-1 Birkeland currents, *Geophys., Res. Lett.*, *10*, 753, 1983.

Carlson, C. W., et al., The FAST mission, *Geophys. Res. Lett.*, in press, 1998.

Ergun, R. E., et al., FAST satellite observations of electric field structures in the auroral zone, *Geophys. Res. Lett.*, in press, 1998a.

Ergun, R. E., et al., FAST satellite observations of large amplitude solitary waves, *Geophys. Res. Lett.*, in press, 1998b.

Evans, D. S., Precipitation electron fluxes formed by a magnetic-field-aligned potential difference, *J. Geophys. Res*, 79, 2852, 1974.

Gorney, D., J., Y. T. Chiu, and D. R. Croley, Jr., Trapping of ion conics by downward parallel electric fields, *J. Geophys. Res.*, *90*, 4205, 1985.

Ijima, T., and T. A. Potemra, Large-scale characteristics of field-aligned currents associated with substorms, *J. Geophys. Res.*, *83*, 599, 1978.

Klumpar, D. M., and W. J. Heikkila, Electrons in the ionospheric source cone: evidence for runaway electrons as carriers of downward Birkeland currents, *Geophys. Res. Lett.*, *9*, 873, 1982.

Klumpar, D. M., Statistical distributions of the auroral electron albedo in the magnetosphere, in Auroral Plasma Dynamics, *Geophsy. Monogr. Ser.*, Vol. *80*, edited by Robert L. Lysak, p. 163, AGU, Washington, DC, 1993.

Marklund, G., L. Blomberg, C.-G. Falthammar, and P.-A. Lindqvist, On intense diverging electric fields associated with black aurora, *Geophys. Res. Lett.*, *21*, 1859, 1994.

McFadden, J. P., et al., Spatial structure and gradients of ion beams observed by FAST, *Geophys. Res. Lett.*, in press, 1998.

Moebius, E., et al., Species dependent energies in upward directed ion beams over auroral arcs as observed with FAST TEAMS, *Geophys. Res. Lett.*, in press, 1998.

Mozer, F. S., et al., Observations of paired electrostatic shocks in the polar magnetosphere, *Phys. Rev. Lett.*, *38*, 292, 1977.

Redsun, M. S., M. Temerin, F. S. Mozer, M. H. Boehm, Classification of auroral electrostatic shocks by their ion and electron associations, *J. Geophys. Res.*, *90*, 9615, 1985.

Shelley, E. G., R. D. Sharp, and R. G. Johnson, Satellite observations of an ionospheric acceleration mechanism, *Geophys. Res. Lett.*, *3*, 654, 1976.

Temerin, M., M. H. Boehm, and F. Mozer, Paired electrostatic shocks, *Geophys. Res. Lett.*, *8*, 799, 1981.

C. W. Carlson, R. E. Ergun, J. P. McFadden, F. S. Mozer, W. Peria, M. Temerin, Space Sciences Laboratory, University of California, Berkeley, CA 94720. (e-mail: cwc; ree; mcfadden; mozer; peria; temerin: @ssl.berkely.edu)

D. Klumpar, E. Shelly, W. Peterson, Lockheed Martin Palo Alto Res. Lab., Palo Alto, CA 94304. (e-mail: klump@agena.space.lockheed.com)

E. Moebius, Morse Hall, University of New Hampshire, Durham, NH 03824. (e-mail: eberhard.moebius@unh.edu)

R. Elphic, Los Alamos National Laboratory, D438, Los Alamos, NM 87545. (e-mail: relphic@lanl.gov)

R. Strangeway, IGPP, University of California, Los Angeles, CA 90095. (e-mail: stranga@igpp.ucla.edu)

C. A. Cattell, Tate Laboratory of Physics, University of Minnesota, Minneapolis, MN 55455. (e-mail: cattell@belka.spa.umn.edu)

R. Pfaff, NASA Goddard Space Flight Center, Code 696, Greenbelt, MD 20771. (e-mail: rob.pfaff@gsfc.nasa.gov)

(Received January 19, 1998; accepted February 16, 1998.)